Flapping wings in line formation flight: a computational analysis

M. Ghommem
mehdig@vt.edu
Center for Numerical Porous Media (NumPor)
King Abdullah University of Science and Technology (KAUST)
Saudi Arabia

V. M. Calo
Center for Numerical Porous Media (NumPor)
Applied Mathematics & Computational Science and Earth Sciences & Engineering
King Abdullah University of Science and Technology
Saudi Arabia

ABSTRACT

The current understanding of the aerodynamics of birds in formation flights is mostly based on field observations. The interpretation of these observations is usually made using simplified aerodynamic models. Here, we investigate the aerodynamic aspects of formation flights. We use a potential flow solver based on the unsteady vortex lattice method (UVLM) to simulate the flow over flapping wings flying in grouping arrangements and in proximity of each other. UVLM has the capability to capture unsteady effects associated with the wake. We demonstrate the importance of properly capturing these effects to assess aerodynamic performance of flapping wings in formation flight. Simulations show that flying in line formation at adequate spacing enables significant increase in the lift and thrust and reduces power consumption. This is mainly due to the interaction between the trailing birds and the previously-shed wake vorticity from the leading bird. Moreover, enlarging the group of birds flying in formation further improves the aerodynamic performance for each bird in the flock. Therefore, birds get significant benefit of such organised patterns to minimise power consumption while traveling over long distances without stop and feeding. This justifies formation flight as being beneficial for bird evolution without regard to potential social benefits, such as, visual and communication factors for group protection and predator evasion.

Paper No. 4062. Manuscript received 12 September 2013, revised version received 18 December 2013, accepted 21 December 2013.

https://doi.org/10.1017/S0001924000009325 Published online by Cambridge University Press

NOMENCLATURE

A	wing's area
$\mathbf{A}$	influence matrix
A_ϕ	amplitude of the flapping angle
b	wing's span
c	wing's chord
C_L	lift coefficient
C_P	power coefficient
C_T	thrust coefficient
F_X	tangential aerodynamic force
F_Z	normal aerodynamic force
K_{decay}	decay parameter controling the wake decay mechanism
L	lift force
N	number of birds in the formation
N_{ts}	number of time steps per flapping cycle
P	aerodynamic power
T	thrust force
U_∞	freestream velocity
V	velocity
$(x_{rel}; y_{rel})$	relative position between leading and trailing birds
$\overline{(.)}$	time-averaged quantity over a flapping cycle

Greek symbols

φ	flapping angle
Γ	vorticity circulation
η	propulsive efficiency
κ	reduced frequency
θ	distortion angle
ρ	fluid density
ω	flapping frequency

Subscripts

$wi - wi$	wing
$wa - wa$	wake
n	normal component
te	trailing edge

Superscripts

$wi - wi$	wing-wing influence
$wa - wi$	wake-wing influence
t	time
Δt	time-step

https://doi.org/10.1017/S0001924000009325 Published online by Cambridge University Press

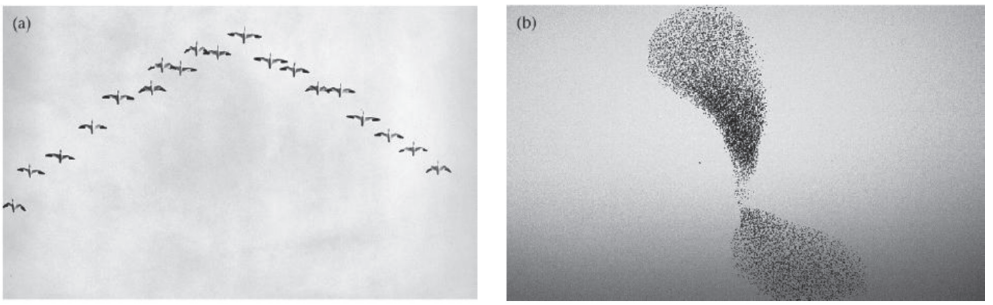


Figure 1. Line formation of snow geese, *Chen hyperborea* (left).
Cluster formation of European starlings, *Sturnus vulgaris* (right). (2009 STARFLAG project, INFMCNR)

1.0 INTRODUCTION

Self-organisation is a well-established property of nature that occurs in several biological systems, such as fish joining together in schools and birds flying in line and cluster formations (see Fig. 1). In the latter organised systems, a global pattern arises from the interactions between each component. The general understanding of these interactions and aerodynamics mechanisms involved in such organised flights is based on field observations[1-6] and their interpretation using simplified aerodynamic models[7-12]. In Ref. 2, Weimerskirch *et al* recorded heart rates of birds as a surrogate of the energy expenditure in a group of eight great white pelicans trained to fly in V-shaped formation. They found that, when in formation, birds had a heart rate of 11·4%-14·5% lower than in birds flying alone and they observed that pelicans beat their wings less frequently and glide for longer periods when flying in a group. Based on a rough calculation of flight energy expenditure, they estimated a total energy saving of 11·4%-14% being achieved when flying in formation. In their studies based on radar measurements made on two species, namely red knots and dunlins[13], they were observed to fly 5km per hour faster in flocks than when they were flying alone; that is, about 8% increase with respect to their average speed in solo flight.

The aerodynamic benefits of formation flights have been recognised and explained. For instance, several aerodynamic studies[7-12] have shown that a trailing bird flying in the upwash region of the wake vortices shed by the leading bird may undergo a forward tilted lift vector which yields a reduction in the induced drag and increase in the lift. Consequently, the trailing bird may fly at a lower angle of attack than the leading one while maintaining the same lift. This results in savings in the energy expenditure. Flapping wings in formation flight may encounter and interact with the wake created by other wings during previous cycles. This phenomenon is referred to as wake capture. Sane and Dickinson[14] and later Birch and Dickinson[15] investigated experimentally this unsteady effect in the context of hovering flight. They compared the experimental force measurements data from a dynamically scaled robotic insect-like model with those obtained from quasi-steady models to isolate and quantify the aerodynamic influence of the wake. Their results demonstrate a significant role of the wake capture in the lift generation. Ansari *et al*[16] pointed out that the wake shed behind a flapping wing contains energy provided to the surrounding fluid in the form of momentum and heat. Thus, the flapping wing might get back some of this energy and use it to improve its flight performance. As such, Grodnitsky and Morozov[17] suggested that birds use particular mechanisms to extract energy back from the near vortex wake.

https://doi.org/10.1017/S0001924000009325 Published online by Cambridge University Press

Recently, there has been a great interest in the modelling and numerical simulation of formation flights inspired by mimicking birds[18-22]. Different aerodynamic models ranging from single horseshoe vortex-based methods[23] to panel methods[8,18,24] have been proposed and used to analyse fixed and flapping wings in formation flights. Lissaman and Shollenberger[7] performed a quantitative analysis, based on simple aerodynamic theories, to come up with a rough estimation of the amount of energy saved by a group of birds flying in a V-shape formation. They showed that a group of 25 birds flying together in formation could achieve an energy decrease of 71% as compared to a single bird in solo flight. Energy saving in formation flight has been also recently examined by Willis *et al*[25]. They used a potential flow solver that assumes rigid wake shapes and does not account for inter-wake influences. This may not be representative of the complex vortex-vortex interactions which take place in formation flight. They found that optimal energy savings can be achieved when the wakes of the leading and trailing flapping wings are in spatial phase. Clearly, migratory birds, which usually fly for long distances without stop and feeding, get benefit from grouping arrangement to carefully manage flight energy consumption.

Other studies based on field observations[26-29] have suggested social and perceptual factors as potential reasons for organised flights in line formation, in particular when arranged in V-shape. Such arrangement was observed to enable a good visibility of the neighbors and a clear visual field to the front. In fact, birds may have a limited amount of binocular vision to the front. As such, a V-angle of 58º or greater let every bird in the formation to see each other, even those following behind[29]. In a recent review paper[30], Bajec and Heppner presented the current state-of-art of the studies made on organised flights. They summarised the reported field observations along with their interpretations of birds in line and cluster formations. All these observations of such fascinating phenomena motivate the computational assessment of the associated aerodynamic aspects. We seek to improve the understanding of the flight formation physics. This will provide guidance for the development of new unmanned air vehicles designed to conduct missions involving close proximity formation flights, multi-vehicle interaction and co-operation[23,31].

In this paper, we conduct a computational study of flapping wings in line formation flight to discern the associated aerodynamic mechanisms. Towards this end, we use the three-dimensional version of the unsteady vortex lattice method (UVLM) to simulate the flow over flapping wings and evaluate the aerodynamic forces and power. UVLM has the capability to capture unsteady effects associated with the previously-shed wake vorticity, as well as wake-capture effects, both of which present important aerodynamic aspects in formation flights. Several research efforts have concluded favorably as to the appropriateness of UVLM for preliminary flapping wing design studies for cruise configurations where there is no flow separation nor substantial wing-wake interactions[32-39]. In a recent paper, Persson *et al*[38] showed through a detailed comparison between UVLM and higher-fidelity computational fluid dynamics simulations for flapping flight that the UVLM schemes produce accurate results for attached flow cases and even remain trend-relevant in the presence of flow separation.

In this work, we demonstrate the importance of the unsteady wake effects in offering power saving and significant increase in lift and thrust generation for flapping wings in line arrangement. We also analyse the effect of wing shape on their aerodynamic performance. Furthermore, we study the effect of group size. Of interest, enlarging the number of flyers in a flock was observed to enable superior global performance.

The remainder of the paper is organised as follows: first, the aerodynamic model used to simulate flapping wings in formation flights is described. Then, the results obtained for different wing shapes and formation flight configurations are reported and observations of their effects on the flapping flight performance are presented. The work concludes with a discussion of the main results on the physics of formation flight and recommendations are drawn.

https://doi.org/10.1017/S0001924000009325 Published online by Cambridge University Press

2.0 AERODYNAMIC MODELLING

A potential flow solver based on the unsteady vortex lattice method (UVLM) is used for the prediction of the unsteady aerodynamic forces and moments. This allows us to investigate the interactions between flapping wings in formation flight and determine the interaction effect on flight efficiency in terms of generation of aerodynamic loads and power consumption in formation-flight configurations. UVLM computes the loads generated by pressure differences across the wing surface that account for unsteady effects such as added mass forces, the growth of bound circulation, and the wake. UVLM applies only to an ideal fluid in incompressible, inviscid, and irrotational flows where the separation lines are known *a priori*. Thus, UVLM requires the fluid to leave the wing smoothly at the trailing edge through imposing the Kutta condition.

The UVLM solver includes the following steps[35]:

- The wing surface is discretised into a lattice of vortex rings. Each vortex ring consists of four short straight vortex segments, with a collocation point placed at the ring's centre.
- A no-penetration condition is imposed at the collocation points. That is, the normal component of the velocity, due to wing-wing and wake-wing interactions, as well as free-stream velocities, is assumed to vanish at each collocation point. Using the Biot-Savart law to compute velocities in terms of vorticity circulations Γ yields a linear system of equations that can be expressed as:

$$A^{wi-wi}\Gamma^{wi} = -A^{wa-wi}\Gamma^{wa} + V_n \qquad \ldots (1)$$

  where A^{wi-wi} and A^{wa-wi} are wing–wing and wake–wing influence matrices, respectively. The vector $\mathbf{V_n}$ collects the normal component to the wing surface of the velocity at each collocation point due to the wing motion. The vectors $\mathbf{\Gamma^{wi}}$ and $\mathbf{\Gamma^{wa}}$ stand for the circulations of the vortex elements on the wing and wake, respectively[34,35].
- Vorticity is introduced to the wake by shedding vortex segments from the trailing edge. These vortices are moved with the fluid particle velocity and their individual circulations are initially equal to that obtained at the trailing edge at the previous time step (i.e., $\Gamma_0^{wa}(t+\Delta t) = \Gamma_{te}^{wi}(t)$ where the subscript *te* stands for the trailing edge). In real flight situations, the circulation of the wake vortex segments decays with time as a manifestation of viscous dissipation. As such, we model the wake vortex strength decay as in Refs 33 and 40.

$$\begin{aligned}\Gamma^{wa}(t) &= \Gamma_0^{wa}(t)\mu(t) \\ &= \Gamma_0^{wa}(t)\sqrt{K_{decay}/[(U_\infty(t-t_s)/c) + K_{decay}]}\end{aligned} \qquad \ldots (2)$$

  where Γ_0^{wa} is the initial value of circulation (when first shed from the trailing edge into the wake), t_s is time at which the vortex segment was convected into the wake, c is the chord length, U_∞ is the freestream velocity, and K_{decay} is a constant parameter that controls the wake decay mechanism. Smaller values of K_{decay} provide more attenuation of the effect of the wake on the flight performance. The wake decay model, given by Equation (2), was first proposed by Leishman[40] in the context of aerodynamic simulation of helicopter blades. Later, Fritz and Long[33] adopted the same model to simulate flapping flights. The effect of the wake decay mechanism on the aerodynamic performance of flapping wings in forward flights is addressed in the next section. As the wing-wake interactions between multiple wings flying in formation present an important feature, all wake vortex rings are considered.

https://doi.org/10.1017/S0001924000009325 Published online by Cambridge University Press

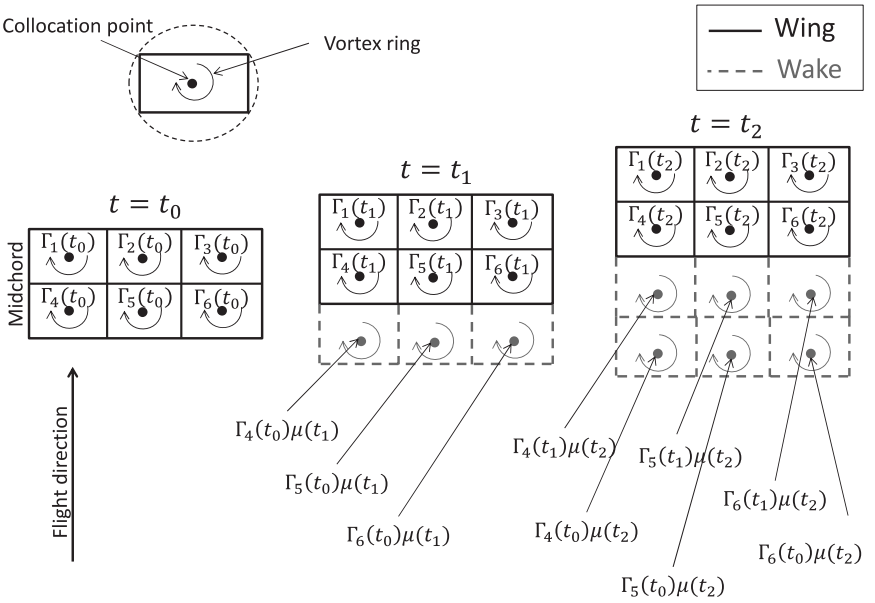


Figure 2. Vortex lattice sheets that model the boundary layer at the lifting surface (wing) and its wake at the first three time steps.

Figure 2 illustrates the shedding mechanism of the wake. It plots a 2 x 3 lattice that models half a wing at the first time steps. The flow is symmetric about the center chord plane of the wing. At $t = t_0$, there is no wake vorticity yet. At $t = t_1$, the vorticity starts to shed from the trailing-edge and yields the first row of wake vortices. The same mechanism is carried out for the next time steps.

- The pressure is evaluated at each collocation point based on the unsteady Bernoulli equation and then integrated over the wing surface to compute the aerodynamic forces and power. The lift (perpendicular to the freestream direction) and thrust (parallel to the freestream direction) coefficients along with the aerodynamic power and the propulsive efficiency (defined as the ratio of the propulsive power over the aerodynamic power[35]), are defined as:

$$C_L = \frac{F_Z}{0{\cdot}5\,\rho\,U_\infty^2\,c\,b}$$
$$C_T = \frac{F_X}{0{\cdot}5\,\rho\,U_\infty^2\,c\,b}$$
$$C_P = \frac{P}{0{\cdot}5\,\rho\,U_\infty^3\,c\,b} \qquad \ldots (3)$$
$$\eta = \frac{\overline{C}_T}{\overline{C}_P}$$

where F_Z and F_X are the aerodynamic forces along the normal and tangent directions (with respect to the freestream direction), P is the required power input, b is the wing span length. The overline denotes averaged values over one flapping cycle. In this work, the power P is

https://doi.org/10.1017/S0001924000009325 Published online by Cambridge University Press

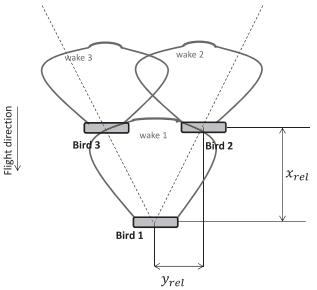


Figure 3. Formation flight configuration — top view (three avian-like flapping wings). The relative position between the leading bird and the trailing bird is defined by (x_{rel}; y_{rel}).

computed as the numerical integration of the normal force to the wing surface dotted with the velocity due to the forward and flapping motions over the wing surface[34,35]. The power P accounts only for the aerodynamic contribution. The inertial power input required to flap the wings is ignored. This assumption remains reasonable for forward flights[41]. For more details on the current implementation of UVLM along with verification and validation studies, the reader is referred to Refs 35, 42 and 43.

- Following our work on resolution independent UVLM simulation[43], particular care was taken when selecting the mesh and time step sizes to obtain accurate prediction of the aerodynamic loads. We observed that UVLM may fail to converge under mesh refinement when the time step size is not selected properly. Thus, to remove mesh sensitivity from UVLM simulations, we proposed to first determine the appropriate time step in order to achieve convergence of UVLM simulations when refining the aerodynamic mesh. This selection approach has been followed to achieve invariant UVLM simulation results under mesh refinement.

Modelling of formation flight

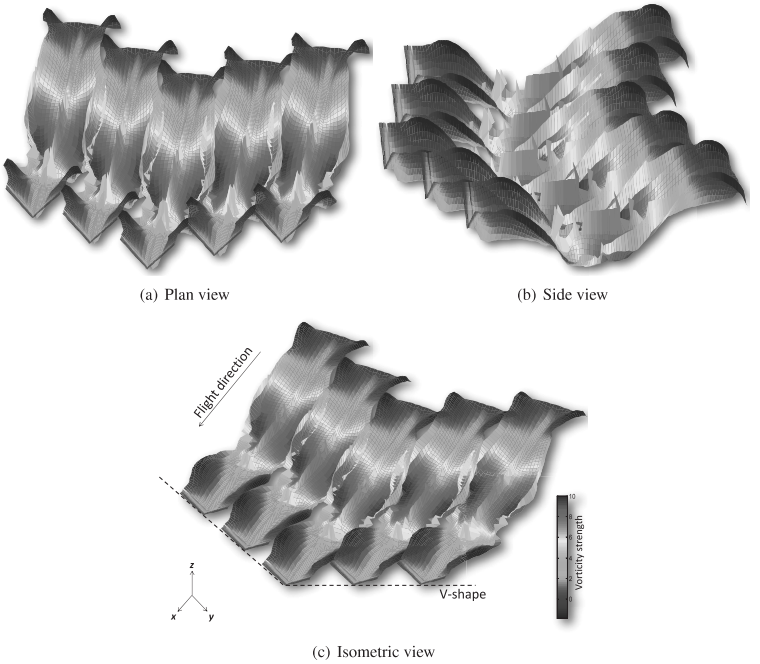
The modifications required to model the interactions of multiple wings and wakes are introduced to the matrix system obtained when imposing the no-penetration condition as follows:

$$\begin{pmatrix} A_{11}^{wi-wi} & \cdots & A_{1N}^{wi-wi} \\ \vdots & \ddots & \vdots \\ A_{N1}^{wi-wi} & \cdots & A_{NN}^{wi-wi} \end{pmatrix} \begin{pmatrix} \Gamma_1^{wi} \\ \vdots \\ \Gamma_N^{wi} \end{pmatrix} = -\begin{pmatrix} A_{11}^{wa-wi} & \cdots & A_{1N}^{wa-wi} \\ \vdots & \ddots & \vdots \\ A_{N1}^{wa-wi} & \cdots & A_{NN}^{wa-wi} \end{pmatrix} \begin{pmatrix} \Gamma_1^{wa} \\ \vdots \\ \Gamma_N^{wa} \end{pmatrix} + V_n \quad \ldots (4)$$

where Γ_i^{wi} and Γ_i^{wa} denote each element i of the vector collecting the circulation of the vortex elements of the wing and wake, respectively. For the influence matrices, A_{ij}^{wi-wi} refers to the effect of wing i on wing j and A_{ij}^{wa-wi} refers to the effect of wake i on wing j. V_n collects the normal component of the velocity at each collocation point of all wings. We account for the interactions between the wakes when convecting the vortex segments. At each time step, to update the position of the wakes, we compute the local particle velocity of each point of the wake vortex rings while including the effect of the freestream and all of the bound and free wake sheets.

In Fig. 3, we show three avian-like flapping wings in symmetric V-formation flight. The relative position between the leading bird and the trailing bird is defined by (x_{rel}; y_{rel}). In the subsequent

https://doi.org/10.1017/S0001924000009325 Published online by Cambridge University Press



(a) Plan view (b) Side view

(c) Isometric view

Figure 4. Wake patterns of the flapping wings in formation flight. Contour color levels denote the vorticity strength of the wing and the wake. No wake decay is accounted for.

analysis, x_{rel} is chosen so that the following wing flaps in proximity of the leading wings and then interacts with the leader's wake within a short time frame.

In Fig. 4, we plot flapping wings in formation flight and their associated wakes where the colour levels denote the vorticity circulation strength. No wake decay is accounted for in the figure. The vorticity in the wake was generated on and shed from the wing at an earlier time. Thus, examining the wake pattern and vorticity distribution can be helpful to gain insight into the generation of aerodynamic quantities. Pockets of highest circulation are observed in the wake aft of flapping wings during the downstroke. Clearly, the trailing flapping wings interact with the wake shed from the leading ones and then can take advantage of this aerodynamic aspect to improve their performance as discussed in Section 3.

Limitations of the model

UVLM does not account for viscous effects and is unable to properly model the cases of flow separation at the leading-edge and extreme situations where strong wing-wake interactions take place. For instance, if a shed wake ring collides with the leading edge of the trailing wing, UVLM may fail to quantify the resulting pressure distribution over the trailing wing. For this reason, the three-dimensional version of UVLM cannot handle hovering flights except in case of a special treatment of the leading-edge separation based on empirical/ad-hoc models as reported recently by Roccia *et al*[44]. In spite of these restrictions, the use of UVLM remains adequate for the application of our interest[32-34]. Lastly, our present analysis does not account for wing deformability nor for the fluid-structure interaction.

https://doi.org/10.1017/S0001924000009325 Published online by Cambridge University Press

3.0 MULTI-FLAPPING WING FORMATION FLIGHT: RESULTS AND DISCUSSION

3.1 Flapping wing model

In this section, we present results of flapping wings interacting with an incompressible uniform flow and flying in line formation. Each wing has a rectangular shape with an aspect ratio of six and a NACA 83XX cross-sectional profile as studied previously by Ghommem et al[35] unless stated otherwise. The indication of the last two digits of the NACA profile, describing the wing thickness, is irrelevant for our study since the current implementation of UVLM assumes a thin wing. As observed in nature[2-5], birds flying in line formation follow an organised pattern in V-shape. As such, we consider three avian-like flapping wings in symmetric V-formation flight as shown in Fig. 3. The flapping motion about the wing root (identical for all wings) is assumed symmetric and prescribed as:

$$\varphi(t) = A_{\varphi}\mathrm{Cos}(\omega\, t) \qquad \ldots (5)$$

where φ is the flapping angle and the flapping amplitude A_{φ} is set equal to 45°. The wing root is placed at a fixed angle-of-attack (pitch) of 5° and a reduced frequency equal to 0·1 is used. The reduced frequency is defined as

$$\kappa = \frac{\omega}{U_{\infty}}\frac{c}{2},$$

where ω is the flapping frequency. The wing shape and flapping configuration adopted in the present study are representative of large bird flights[45]. As described in Ref. 43, particular care as taken when selecting the mesh and time step sizes. Each flapping wing is discretised into 10 panels along the spanwise direction and 24 chordwise panels, providing N x 240 vortex rings for the UVLM solver, where N is the number of wings. A small time step of $\Delta t = 2\pi/(120\omega)$ is selected (i.e., 120 time steps per flapping cycle). Under this setting, the aerodynamic quantities were observed to converge. For three wings flying in formation, the total time taken by a workstation featuring Intel Xeon CPU X5650 2.67 GHZ processor to run the aerodynamic solver (implemented in Fortran) for one flapping cycle is 10min 34s. Clearly, the execution time associated with the UVLM solver along with its capability to capture the unsteady effects of the wake make this aerodynamic tool a good candidate to analyse the behaviour and performance of multiple flapping wings flying in close proximity.

As for modelling the wake decay effect, we adopt the model given by Equation (2) and set K_{decay} equal to 20. This value is chosen so that the circulation of the oldest wake rings after one flapping cycle is reduced from its initial value (when first shed from the trailing edge into the wake) by approximately 50%. The baseline cases of the present study correspond to a single flapping vehicle isolated from any interaction with other wings with and without wake decay. The lift-thrust plots obtained for the baseline cases are shown in Fig. 5. Clearly, most of the useful lift and thrust are produced during the downstroke phase. We observe that the lift remains positive during almost the entire stroke. This is mainly due to the positive effective angle of attack resulting from the wing camber and the fixed pitch angle of the wing root set equal to 5°. The generation of the aerodynamic loads is slightly affected when introducing the wake decay mechanism. The averaged values of the lift, thrust, and aerodynamic power coefficients along with the propulsive efficiency obtained for the baseline cases are given in Table 1. The wake decay has minor influence on the

https://doi.org/10.1017/S0001924000009325 Published online by Cambridge University Press

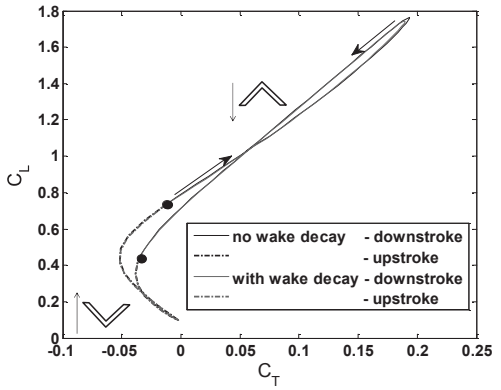


Figure 5. Lift coefficient *vs* thrust coefficient obtained for the baseline cases (flapping wings in solo flight) with and without wake decay. Solid lines denote the downstroke phase and dashed lines denote the upstroke phase. Arrows are introduced to show the variations of the lift and thrust along the two phases of the flapping cycle.

generation of aerodynamic loads and power. This can be explained by the fact that the oldest wake vortex rings, which are most affected by the wake decay mechanism, are far away from the wing and then have little effect on the right-hand side of Equation (4). As such, the effects of the wake decay mechanism is ignored in the subsequent analysis.

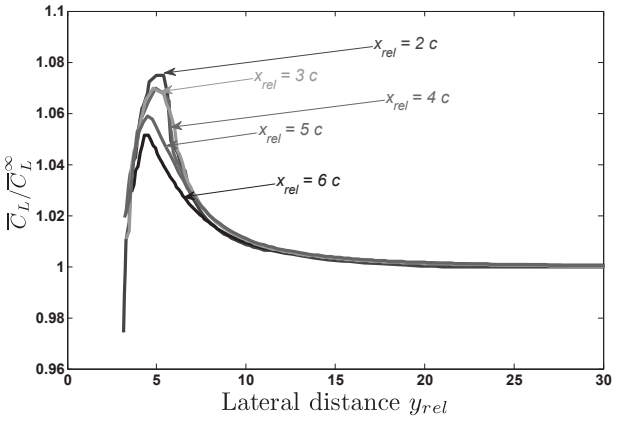
3.2 Flapping wings in formation flights

We examine the effect of the relative position between the leading bird and the trailing bird on the aerodynamic performance of the latter bird. In Fig. 6(a), we plot the variations of the ratio $\overline{C}_L / \overline{C}_L^{\infty}$ with the lateral spacing distance y_{rel} for different values of x_{rel}, where the superscript 1 refers to the aerodynamic quantity obtained for the baseline case (solo flight). The range of variations of y_{rel} was selected so that the wings of Birds 2 and 3 shown in Fig. 3 do not intercept. Clearly, Bird 2 flying behind the leading Bird 1 generates more lift force than achieved when flying alone. As a result, the flapping wings of Bird 2 can be placed at a lower angle of attack or beat at lower frequency than the leading one while still maintaining the same lift, resulting in decreased energy expenditure. We observe a maximum increase of lift of 7·5%, 6·8%, 6·5%, 6%, and 5% c when placing the trailing bird at the relative position (along the x-axis) $x_{rel} = 2$; 3; 4; 5; and 6c, respectively. The lateral spacing distance y_{rel} that corresponds to these maxima is equal to 5·4, 5, 4·9, 4·5, and 4·3 for $x_{rel} = 2$; 3; 4; 5; and 6c, respectively. Beyond those spacing distances, as Bird 2 moves outboard relative to Bird 1, the interaction effect is damped and the lift ratio tends to one (i.e., returns to the amount of lift obtained when flying alone). Clearly, the trailing bird gets benefit of being in proximity of the leading bird (within a specific arrangement in line) to produce more lift.

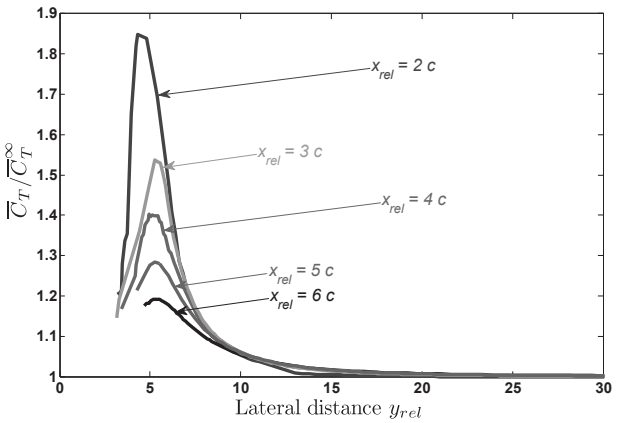
Table 1
Baseline case results: flapping wings in solo flight (rectangular wings). The overline denotes averaged values over one flapping cycle

	Lift coefficient $\overline{C}_L^{\infty}$	Thrust coefficient $\overline{C}_T^{\infty}$	Power coefficient $\overline{C}_P^{\infty}$	Efficiency η
No wake decay	0·755	0·0348	0·1435	0·2428
With wake decay	0·750	0·0339	0·1440	0·2329

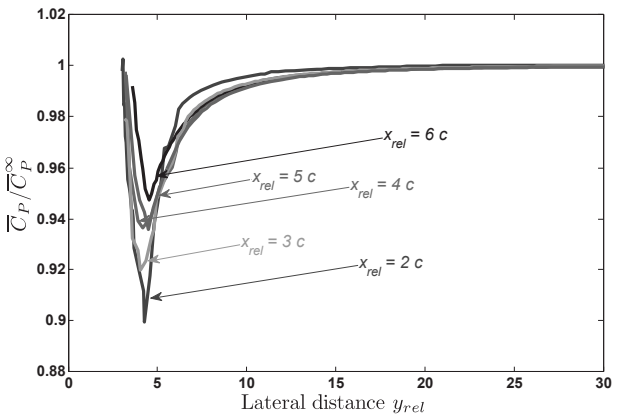
https://doi.org/10.1017/S0001924000009325 Published online by Cambridge University Press



(a) Lift



(b) Thrust



(c) Power

Figure 6. Variations of (a) the lift, (b) thrust, and (c) aerodynamic power ratios with the offset spacing distance y_{rel} (in terms of chord length c). Results are obtained for the trailing birds with rectangular wings when placed at different lateral positions x_{rel} = 2; 3; 4; 5; and 6 c in a symmetric fashion.

https://doi.org/10.1017/S0001924000009325 Published online by Cambridge University Press

In Fig. 6(b), we show the variations of the ratio $\overline{C}_T / \overline{C}_T^{\infty}$ with the lateral spacing distance y_{rel}. A significant increase in the induced thrust is observed when flying in formation. This increase reaches its maximum of 85%, 53%, 40%, 28%, and 30% when placing the trailing bird at the relative position $x_{rel} = 2$; 3; 4; 5; and 6c, respectively. The increase observed in the aerodynamic loads generated by birds flying in close proximity formation can be explained by their interaction with the previously-shed wake of the leading bird. In fact, a trailing bird flying in the region of the wake vortices left by the leading bird experiences a forward tilted lift vector which, effectively reduces the induced drag of the trailing bird while simultaneously increasing its lift.

The variations of the power ratio $\overline{C}_P / \overline{C}_P^{\infty}$ with the lateral spacing distance y_{rel} are shown in Fig. 6(c). Flying in formation enables a power saving that reaches its maximum of 10%, 8%, 6·5%, 6·3%, and 5% when placing the trailing bird at the lateral position $x_{rel} = 2$; 3; 4; 5; and 6c, respectively. Clearly, reducing the value of the relative position x_{rel} (i.e., placing the trailing bird closer to the leading bird) increases the aerodynamic loads and reduces the required power. As would be expected, isolating the flapping wings from interacting with other wings and wakes (i.e., increasing the spacing distance y_{rel}), the power ratio tends to one. The trailing birds, by intercepting the wake generated of the wing trailing edges and tips of the leading bird (see Fig. 4), recapture energy lost to the wake. This phenomenon is usually referred as wake capture which is a well-established mechanism observed in hovering flights of insects and humming birds[14,46,47]. The wake shed behind a flapping wing contains energy provided to the surrounding fluid in the form of momentum and heat. So, the flapping wing gets back some of this energy and employs it to improve its flight performance in terms of power consumption and lift generation.

To gain insight into the reasons why formation flight improves the performance of the trailing flapping wings when properly placed behind the leading wings as can be inferred from Fig. 6, we examine the wake pattern and vorticity distribution. The vorticity circulation strength of the wakes obtained for flapping wings in solo and formation flights is shown in Fig. 7. We observe that the overall strength of the wake has increased in comparison with the baseline case (solo flight), as the average lift and thrust have increased as shown in Fig. 6. Since vorticity in the wake was generated on and shed from the wing at an earlier time, the highest vorticity circulation is achieved during the downstroke. As such, most of the useful aerodynamic loads are obtained during this phase of the flapping cycle. Furthermore, the wake shed from the flapping wings in formation flight is deformed by the interaction with the other wings and wakes.

3.3 Effect of wing shape

To check further the importance of the birds organisation when flying in formation, we perform similar analysis while considering a different wing shape (see Fig. 8). This shape was obtained from an optimisation study performed on flapping wings in solo forward flights[43]. The optimisation analysis combines the B-spline parametrisation which represents the standard technology for describing geometries in computer-aided design (CAD), the UVLM, and a gradient-based optimisation tool. The objective was to identify a set of optimal shapes that maximise the propulsive efficiency under several constraints and the baseline flapping model was the same one as the one

Table 2
Baseline case results: flapping wings in solo flight[22]

Lift coefficient	Thrust coefficient	Power coefficient	Efficiency
$\overline{C}_L^{\infty}$	$\overline{C}_T^{\infty}$	$\overline{C}_P^{\infty}$	η
0·911	0·0934	0·197	0·4729

https://doi.org/10.1017/S0001924000009325 Published online by Cambridge University Press

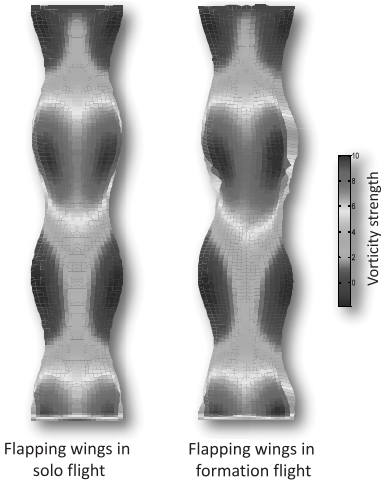


Figure 7. Wake patterns of the flapping wings in solo flight (left) and formation flight (right) — top view. Contour colour levels denote the vorticity strength of the wing and the wake. The flapping wings of the trailing bird in formation flight are located in left behind the leading bird.

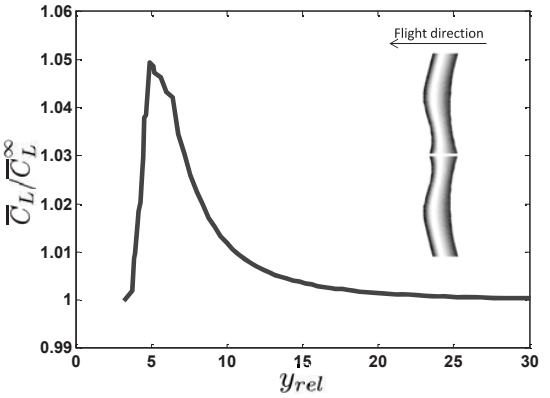
considered in the present study. The averaged values of the lift, thrust, and aerodynamic power coefficients and efficiency obtained for the wing shape shown in Fig. 8 are presented in Table 2. In comparison with the rectangular wing case (as reported in Table 1), an increase of 100% in the efficiency has been reached. This indicates the importance of the shape selection for the performance of flapping wings in forward flight.

We investigate the effect of the wing shape on the aerodynamic performance when varying the V-shape arrangement. In Fig. 8, we show the variations of the lift, thrust, and aerodynamic power ratios with the lateral spacing y_{rel}. The trailing birds are placed at the relative position $x_{rel} = 4c$. Similar trends are observed; that is, the existence of an optimal spacing that yields a maximum increase in the lift and thrust and reduction in the aerodynamic power. In comparison with the rectangular wing case, more power saving is obtained (a reduction of 9%) while lower increases in the lift and thrust are achieved.

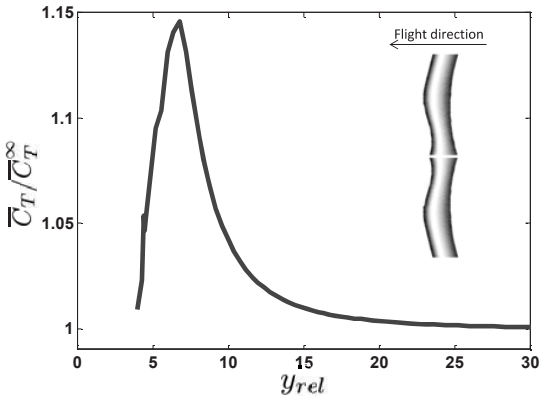
3.4 Effect of group size

We consider a larger group of birds in formation flight as shown in Fig. 9. In this case, we simulate a flock of seven birds. Each bird has a rectangular wing with an aspect ratio of six and a NACA 83XX cross-sectional profile. As for the birds placement, we use the optimised lateral spacing distances obtained for $x_{rel} = 4c$. The incremental lift, thrust, power, and efficiency obtained for birds in formation flight as compared to the baseline cases (solo flight) are presented in Table 3. The improvement in the generation of aerodynamic loads and the reduction in the input aerodynamic power are achieved for all birds in formation. The leading bird benefits the least from the formation flight in terms of aerodynamic loads generation and power saving (a finding consistent with the observation reported in Ref. 48) while the trailing birds experience substantial increases in the thrust and efficiency which reach 45·8 % and 55·8%, respectively, for the last row of birds. We introduce the global lift, thrust, power, and efficiency of the bird group summed up across all wings and report the corresponding values in Table 4. A significant improvement of the global aerodynamic performance is observed.

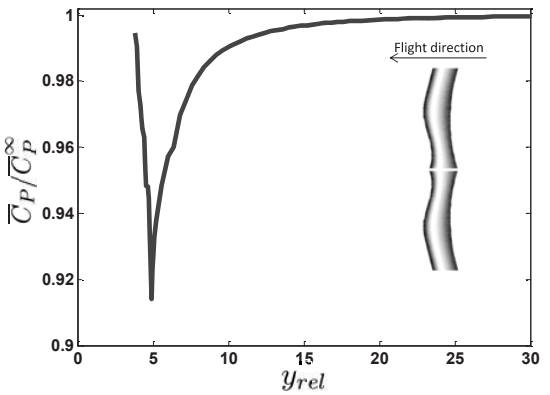
https://doi.org/10.1017/S0001924000009325 Published online by Cambridge University Press



(a) Lift



(b) Thrust



(c) Power

Figure 8. Variations of the (a) lift, (b) thrust, and (c) aerodynamic power ratios with the offset spacing distance y_{rel} (in terms of chord length c). Results are obtained for the trailing birds when placed at $X_{rel} = 4c$ in a symmetric fashion.

https://doi.org/10.1017/S0001924000009325 Published online by Cambridge University Press

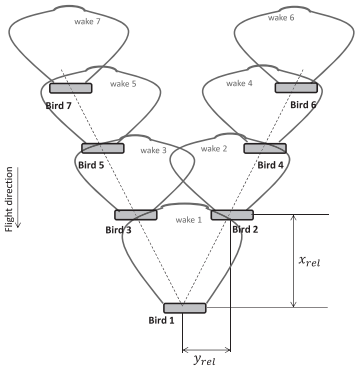


Figure 9. Formation flight configuration — top view (seven avian-like flapping wings). The trailing birds are placed on the dashed line with the same lateral offset distances.

To investigate further the trend observed when increasing the number of birds, we simulate a group of 11 birds flying in formation with the same V-shape as considered previously. This results in a dense linear system, as given by Equation (1), with a dimension of 2,640. The total execution time to run one flapping cycle is 5h 58min 23s. The results show a similar trend where the furthest row of birds experiences an increase in the thrust and efficiency of 52% and 60%, respectively. Clearly, enlarging the group of birds flying in formation improves the aerodynamic performance. This finding is consistent with the conclusion made by Beauchamp[5] who documented 72 evolutionary shifts in migration distance for 409 bird species. The author found that long-distance migration which requires more physical effort, as opposed to short-distance migration, was associated with a larger traveling group size. As such, birds organise themselves in large groups when flying over long distances in order to carefully manage flight energy consumption.

Table 3
Incremental lift, thrust, power, and efficiency obtained for birds in formation flight as compared to the baseline case (solo flight)

	Incremental lift ΔC_L	Incremental thrust ΔC_T	Incremental power ΔC_P	Incremental efficiency $\Delta\eta$
Bird 1 (leading bird)	+ 2·0 %	+ 9·0 %	- 2·5 %	+ 12·5 %
Bird 2-3 (trailing birds)	+ 7·0 %	+ 32·0 %	– 4·4 %	+ 40·4 %
Bird 4-5 (trailing birds)	+ 7·2 %	+ 39·6 %	– 5·1 %	+ 48·7 %
Bird 6-7 (trailing birds)	+ 6·0 %	+ 45·8 %	– 5·2 %	+ 55·8 %

Table 4
Global aerodynamic performance of flapping wings in solo and formation flight (rectangular wings). The overline denotes averaged values over one flapping cycle

	Lift coefficient $\overline{C}_L^{\infty}$	Thrust coefficient $\overline{C}_T^{\infty}$	Power coefficient $\overline{C}_P^{\infty}$	Efficiency η
Solo flight	0·755	0·0348	0·1435	0·2428
Formation flight	0·800	0·0497	0·1368	0·3472

https://doi.org/10.1017/S0001924000009325 Published online by Cambridge University Press

4.0 CONCLUSION

In this work, we use a potential flow solver based on the unsteady vortex lattice method to simulate flapping wings in formation flight. In our simulations, we account for the aerodynamic coupling between flapping wings along with their interactions with the wake vorticity. Our numerical analysis is motivated by field observations of migratory birds. The results show that flying in V-shaped formation at optimal spacing yields significant increase in the lift and thrust and savings in the power consumption. This can be explained by the inherent interaction between the trailing birds and the previously-shed wake vorticity from the leading bird. We also examine the effect of the wake decay on the aerodynamic performance of flapping wings. Little influence of the wake decay on the generation of aerodynamic loads and power is observed. We expect this effect to be more pronounced in cluster formation flights which involve a large number of small birds flying in proximity to each other and operating at higher flapping frequencies. We find that enlarging the group of birds flying in line formation further increases the aerodynamic performance. Thus, without referring to other potential reasons, birds take advantage of organised patterns to minimise power consumption while travelling over long distances without stopping and feeding: a conclusion consistent with the observational data reported by field observations for migratory birds.

REFERENCES

1. BALLERINI, M., CABIBBO, N., CANDELIER, R., CAVAGNA, A., CISBANI, E., GIARDINA, I., ORLANDI, A., PARISI, G., PROCACCINI, A., VIALE, M. and ZDRAVKOVIC, V. Empirical investigation of starling flocks: a benchmark study in collective animal behaviour, *Animal Behaviour*, **76**, 2008, pp 201–215.
2. WEIMERSKIRCH, H., MARTIN, J., CLERQUIN, Y. ALEXANDRE, P. and JIRASKOVA, S. Energy saving in flight formation, *Nature*, 2001, **413**, pp 697-698.
3. CUTTS, C.J. and SPEAKMAN, J.R. Energy saving in formation flight of pink-footed geese, *J Experimental Biology*, 1994, **189**, pp 251-261.
4. SPEDDING, G. The cost of flight in flocks, *Nature*, 2011, **474**, pp 458-459.
5. BEAUCHAMP, G. Long-distance migrating species of birds travel in larger groups, *Biology Letters*, 2011, **7**, pp 692-694.
6. HAINSWORTH, F.R. Induced drag savings from ground effect and formation flight in brown pelicans, *J Experimental Biology*, 1988, **135**, pp 431-444.
7. LISSAMAN, P.B.S. and SHOLLENBERGER, C.A. Formation flight of birds, *Science*, 1970, **168**, pp 1003-1005.
8. SABAN, D. WHIDBORNE, J.F. and COOKE, A. Simulation of wake vortex effects for UAVs in close formation flight, *Aeronaut J*, 2009, **113**, pp 727-738.
9. HAINSORTH, F.R. Precision and dynamics of positioning by Canada geese flying in formation, *J Experimental Biology*, 1987, **128**, pp 445-462.
10. BADGEROW, J.P. and HAINSWORTH, F.R. Energy savings through formation flight? a re-examinationof the vee formation, *J Theoretical Biology*, 1981, **93**, pp 41-52.
11. SEILER, P., PANT, A. and HEDRICK, J.K. A systems interpretation for observations of bird formations, *J Theoretical Biology*, 2003, **221**, pp 279-287.
12. KING, R. and GOPALARATHNAM, A. Ideal aerodynamics of ground effect and formation flight, *J Aircr,* 2005, **42**, pp 1188-1199.
13. NEWTON, I. *The Migration Ecology of Birds*, 2008, Academic Press.
14. SANE, S.P. and DICKINSON, M.H. The aerodynamics effects of wing rotation and a revised quasi steady model of flapping flight, *J Experimental Biology*, 2002, **205**, pp 1087-1096.
15. BIRCH, J.M. and DICKINSON, M.H. The influence of wing wake interactions on the productionof aerodynamic forces in flapping flight, *J Experimental Biology*, 2003, **206**, pp 2257-2272.
16. ANSARI, S.A., ZBIKOWSKI, R. and KNOWLES, K. Aerodynamic modelling of insect-like flappingflight for micro air vehicles, *Prog in Aerospace Sci*, 2006, 42, pp 129-172.
17. GRODNITSKY, D.L. and MOROZOV, P.P. Vortex formation during tethered flight of functionally and morphologically two-winged insects, *J Experimental Biology*, 1993, **182**, pp 11-40.
18. BRAMESFELD, G. and MAUGHMER, M.D. Effects of wake rollup on formation-flight aerodynamics, *J Aircr*, 2008, **45**, pp 1167-1173.

https://doi.org/10.1017/S0001924000009325 Published online by Cambridge University Press

19. NING, A., FLANZER, T.C. and KROO, I.M. Aerodynamic performance of extended formation flight, *J Aircr*, 2011, **48**, pp 855-865.
20. KLESS, J.E., AFTOSMIS, M.J., NING, S.A. and NEMEC, M. Inviscid analysis of extended-formation flight, *AIAA J*, 2013, **51**, pp 1703-1715.
21. GIULIETTI, F., INNOCENTI, M., NAPOLITANO, M. and POLLINI, L. Dynamic and control issues of formation flight, *Aerospace Sci and Tech*, 2005, **9**, pp 65-71.
22. ZOU, Y., PAGILLA, P.R. and RATLIFF, R.T. Distributed formation flight control using constraint forces, *J Guidance, Control, and Dynamics*, 2009, **32**, pp 112-120.
23. BLAKE, W. and MULTHOPP, D. Design, performance and modeling considerations for close formation flight, *Proceedings of the AIAA Atmospheric Flight Mechanics Conference and Exhibit*, 1998, AIAA Paper 98-4343.
24. IGLESIAS, S. and MASON, W.H. Optimum spanloads in formation flight, 2002, AIAA Paper 2002-0258.
25. WILLIS, D.J., PERAIRE, J. and BREUER, K.S. A computational investigation of bio-inspired formation flight and ground effect, *Proceedings of the 25th AIAA Applied Aerodynamics Conference*, 2007, AIAA Paper 2007-4182.
26. HELBING, D. and MOLNA, P. Social force model for pedestrian dynamics, *Physical Review*, 1995, **E 51**, 42824286.
27. HEPPNER, F.H. Avian flight formations, *Bird-Banding*, 1974, **45**, pp 160-169.
28. HEPPNER, F.H. and HAFFNER, J.D. Communication in bird flocks: an electromagnetic model. *Biological and Clinical Effects of Low-Frequency Magnetic and Electric Fields*, 1974, Springfield, IL, USA.
29. HEPPNER, F.H., CONVISSAR, J.L., MOONAN, D.E. and ANDERSON, J.G.T. Visual angle and formation flight in Canada geese (branta canadensis), 1985, *AUK*, **102**, pp 195-198.
30. BAJEC, I.L. and HEPPNER, F.H. Organized flight in birds, *Animal Behaviour*, 2009, **78**, pp 777-789.
31. BLAKE, W.B. and GINGRAS, D.R. Comparison of predicted and measured formation flight interference effects, *J Aircr*, 2004, **41**, pp 201-207.
32. VEST, M.S. and KATZ, J. Unsteady aerodynamic model of flapping wings, *AIAA J*, 1996, **34**, pp 1435-1440.
33. FRITZ, T.E. and LONG, L.N. Object-oriented unsteady vortex lattice method for flapping flight, *J Aircraft*, 2004, **41**, pp 1275-1290.
34. STANFORD, B.K. and BERAN, P.S. Analytical sensitivity analysis of an unsteady vortex-lattice method for flapping-wing optimization, *J Aircr*, 2010, **47**, pp 647-662.
35. GHOMMEM, M., HAJJ, M.R., MOOK, D.T., STANFORD, B.K., BERAN, P.S. and WATSON, L.T. Global optimization of actively-morphing flapping wings, *J Fluids and Structures*, 2012, **30**, pp 210-228.
36. SMITH, M.J.C., WILKIN, P.J. and WILLIAMS, M.H. The advantages of an unsteady panel method in modelling the aerodynamic forces on rigid flapping wings, *J Experimental Biology*, 1996, **199**, pp 1073-1083.
37. GHOMMEM, M., COLLIER, N., NIEMI, A.H. and CALO, V.M. Shape optimization and performance analysis of flapping wings, *Proceedings of The Eighth International Conference on Engineering Computational Technology*, 2012.
38. PERSSON, P., WILLIS, D. and PERAIRE, J. Numerical simulation of flapping wings using a panel method and high-order Navier-Stokes solver, *Int J for Numerical Methods in Engineering*, 2012, **89**, pp 296-1316.
39. GHOMMEM, M., HAJJ, M.R., MOOK, D.T., STANFORD, B.K., BERAN, P.S. and WATSON, L.T. Global local optimization of flapping kinematics in hovering flights, *Int J Micro Air Vehicles*, 2013, **5**, (2), pp 109-126.
40. LEISHMAN, J.G. *Principles of Helicopter Aerodynamics*, 2000, Cambridge Univ Press, Cambridge, UK.
41. SHYY, W., BERG, M. and LJUNGSQVIST, D. Flapping and flexible wings for biological and micro air vehicles, *Prog in Aerospace Sci*, 1999, **35**, pp 455-505.
42. GHOMMEM, M. Modeling and Analysis for Optimization of Unsteady Aeroelastic Systems, PhD thesis, 2011 Virginia Polytechnic Institute and State University, Blacksburg, VA , USA.
43. GHOMMEM, M., COLLIER, N., NIEMI, A.H. and CALO, V.M. On the shape optimization of flapping wings and their performance analysis, *Aerospace Sci and Tech*, in press.
44. ROCCIA, B.A., PREIDIKMAN, S. and MASSA, J.C. Modified unsteady vortex-lattice method to study flapping wings in hover flight, *AIAA J*, 2013, **51**, pp 2628-2642.
45. PENNYCUICK, C.J. Wingbeat frequency of birds in steady cruising flight: New data and improved predictions, *J Experimental Biology*, 1996, **199**, pp 1613-1618.
46. WU, J.H., ZHANG, Y.L. and SUN, M. Hovering of model insects: simulation by coupling equations of motion with Navier-Stokes equations, *J Experimental Biology*, 2009, **212**, pp 3313-3329.
47. GHOMMEM, M., HAJJ, M.R., MOOK, D.T., STANFORD, B.K., BERAN, P.S. and WATSON, L.T. Global local optimization of flapping kinematics in hovering flights, *Int J Micro Air Vehicles*, 2013, **5**, (2), pp 09-126.
48. ANDERSSON, M. and WALLANDER, J. Kin selection and reciprocity in flight formation?, *Behavioral Ecology*, 2004, **15**, pp 158-162.

https://doi.org/10.1017/S0001924000009325 Published online by Cambridge University Press